SCIENCE CHINA
Information Sciences

• LETTER •

May 2024, Vol. 67, Iss. 5, 159403:1–159403:2
https://doi.org/10.1007/s11432-023-3991-9

High-performance carbon-electrode-based self-powered optoelectronic synaptic devices

Wen HUANG[1], Xuwen XIA[1], Huixing ZHANG[1], Tenglong GUO[3], Pengjie HANG[2*], Bin LI[1], Jiawei TANG[1], Biao LI[2], Chen ZHU[3], Lei WANG[3], Deren YANG[2], Xuegong YU[2*] & Xing'ao LI[1*]

[1]*Jiangsu Provincial Engineering Research Center of Low Dimensional Physics and New Energy & School of Science, Nanjing University of Posts and Telecommunications, Nanjing* 210023*, China;*
[2]*State Key Laboratory of Silicon and Advanced Semiconductor Materials, Zhejiang University, Hangzhou* 310027*, China;*
[3]*College of Integrated Circuit Science and Engineering, Nanjing University of Posts and Telecommunications, Nanjing* 210023*, China*

Received 26 December 2023/Revised 10 February 2024/Accepted 25 March 2024/Published online 11 April 2024

A two-terminal self-powered optoelectronic structure could mimic synaptic functions of a human brain synapse unit (Figure 1(a)) based on the photovoltaic effects [1], demonstrating the potential for decreasing energy consumption for future computing. However, current self-powered optoelectronic synaptic devices face issues of stability and cost, which mainly arise from noble metal electrodes and independent hole transport layers used in these structures. Substituting low-cost carbon for these metal electrodes and carrier transport layers may promise to solve these challenges.

Herein, we prepared self-powered Fluorine Doped Tin Oxide (FTO)/Titanium Dioxide(TiO_2)/Methylammonium Lead Triiodide ($MAPbI_3$)/Carbon heterojunction synaptic devices (Figure 1(b)). The detailed information is presented in Appendixes A and B. Important synaptic functions, such as excitatory post-synaptic current (EPSC) as demonstrated in Figure 1(c), paired-pulse facilitation (PPF), spike-number-dependent plasticity (SNDP), and spike-rate-dependent plasticity (SRDP), are well mimicked without an external bias voltage in these devices in response to optical spikes (Appendix C).

The photo-generated electrons and holes of the $MAPbI_3$ layer can efficiently inject into a TiO_2 layer and carbon electrode [2], respectively, owing to their optimal energy-level alignment (Figure 1(d)). To understand the carrier trapping mechanism in the device, X-ray photoelectron spectroscopy (XPS) was employed to confirm the existence of oxygen vacancies in the TiO_2 film (Figure 1(e)). Density functional theory calculation shows that a new band of a defect state is mainly due to the absence of a single oxygen ion within the TiO_2 unit cell occurred just below the Fermi level (Figure 1(e)). The mimicking of synaptic functions probably arises from the electron trapping and de-trapping effects caused by the defect state in the TiO_2 layer (Appendix D).

To demonstrate the self-powered optoelectronic synaptic device performance on the basis of carbon compared with metal electrodes, the storage and operational stability of the carbon-electrode-based synaptic devices and Ag-electrode-based devices were surveyed (Figure 1(f)). It was found that the devices with carbon have almost no attenuation within 672 h under dark storage as reported before [2], but they were completely decayed after less than 100 h with Spiro-OMeTAD/Ag due to the degradation induced by Ag-ion migration into Spiro-OMeTAD [3]. A grey linear fitting line based on their storage stability data for the carbon electrode-based devices is shown in Figure 1(f), demonstrating great storage stability. More importantly, the devices with carbon exhibited significantly higher operational stability than those with Spiro-OMeTAD/Ag, retaining over 70% of their initial power conversion efficiency (PCE) values under continuous 720-hour full-spectrum light illumination with the intensity of $\sim 1\times10^5$ μW/cm^2, which was ∼2400 times the practical optical pulse stimulation in the current work. The results show the stability advantage of self-powered optoelectronic synaptic devices with carbon compared with that with Ag electrodes [4]. Our device structure with such excellent properties inspires us to overcome the high-cost challenge of Au in optoelectronic synaptic device applications as well.

A high optical power of $\sim 1.5\times10^5$ μW/cm^2 was employed to characterize the synaptic currents of the synaptic devices in response to 50 optical pulses for the consistency property investigation. For the device-to-device variation, its variability of the synaptic currents for the ith pulse is quantified by calculating the variation coefficient as the standard deviation divided by the mean current value of the 20 yield devices in the corresponding pulse (Figure 1(g)). The final device-to-device variation is obtained by averaging the variation coefficient at each pulse. The cycle-to-cycle variation was analyzed in the same way by characterizing 100 cycles in a random yield device. The obtained device-to-device and cycle-to-cycle variations were just ∼10% and 6.7% for 20 devices and 100 cycles, respectively (Appendix E).

No external bias voltage is needed in mimicking synaptic functions in these devices, indicating the zero electrical

* Corresponding author (email: hangpengjie@zju.edu.cn, yuxuegong@zju.edu.cn, lixa@njupt.edu.cn)

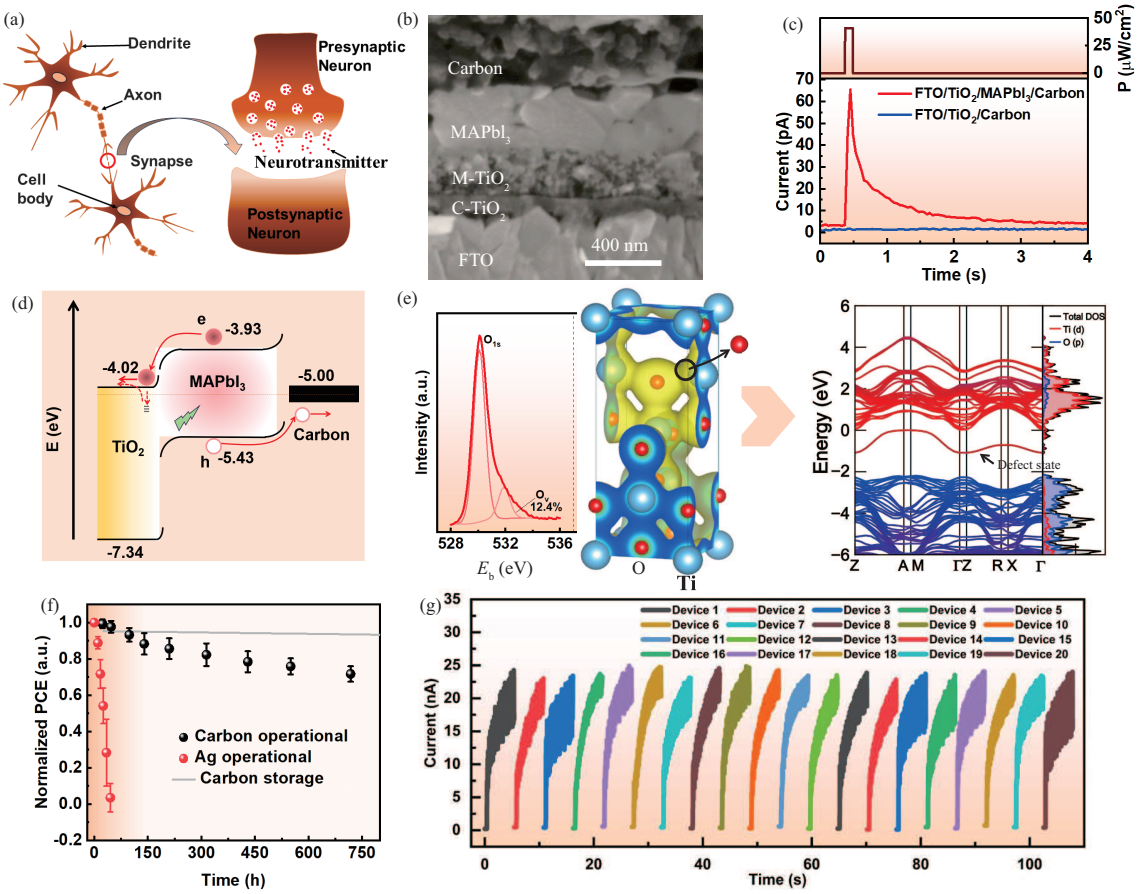

Figure 1 (Color online) (a) Schematics of a biological neural system; (b) a schematic of a cross-sectional scanning electron microscopy image of the synaptic device; (c) synaptic current response of the device stimulated by optical spikes; (d) a schematic of the band alignment and electron/hole behaviors in response to the optical pulse; (e) XPS characterization of the oxygen vacancy in TiO_2 film and its band structure information from the first-principle calculation; (f) normalized power conversion efficiency (PCE) trend of the devices versus time; (g) SNDP behaviors of different yield devices for device-to-device variation study.

energy consumption in driving the carrier transport. The energy is only consumed for an electrical power supply that generates the optical pulse for the stimulation. This means that the energy consumption is related to the needed optical intensity. In the current work, the current device can respond to an optical power density of $\sim 41\times10^5$ μW/cm^2, which is lower than most of the other self-powered optoelectronic synaptic systems; the optical pulse width is 0.05 s, which is lower than all the other self-powered devices. The energy consumption density can be extracted based on the equation of $E_s = P \times t$ ($E_s = P \times S \times t$ / S) [5], in which P indicates the optical power density, t means the optical pulse width, and S is the device area. An ultra-low energy consumption density of $\sim 2.05\times10^3$ nJ/cm^2 is then obtained, which is much smaller than most of the other self-powered systems (Appendix E).

Conclusion. In this study, self-powered optoelectronic synaptic devices with an FTO/TiO_2/$MAPbI_3$/carbon structure were fabricated. The structure well mimicked various typical synaptic functionalities with an ultra-low energy consumption density. It showed high stability and low variation properties based on their PCE behaviors and SNDP synaptic functions in these devices. Our results demonstrate the performance superiorities of the proposed structure arising from the carbon electrodes for the realization of neuromorphic computing in terms of energy consumption, cost, consistency, and stability.

Acknowledgements This work was supported by Natural Science Foundation of Jiangsu Province (Grant Nos. BK20211273, BZ2021031) and National Natural Science Foundation of China (Grant Nos. 62104114, 51872145, 62025403, 62304201, 62090030, 61721005).

Supporting information Appendixes A–E. The supporting information is available online at info.scichina.com and link.springer.com. The supporting materials are published as submitted, without typesetting or editing. The responsibility for scientific accuracy and content remains entirely with the authors.

References

1 Huang W, Hang P J, Wang Y, et al. Zero-power optoelectronic synaptic devices. Nano Energy, 2020, 73: 104790
2 Zhou H, Shi Y, Dong Q, et al. Hole-conductor-free, metal-electrode-free TiO_2/$CH_3NH_3PbI_3$ heterojunction solar cells based on a low-temperature carbon electrode. J Phys Chem Lett, 2014, 5: 3241–3246
3 Liang J J, Li M, Zhu J Y, et al. Detrimental effect of silver doping in spiro-MeOTAD on the device performance of perovskite solar cells. Org Electron, 2019, 69: 343–347
4 Zhu X, Lu W D. Optogenetics-inspired tunable synaptic functions in memristors. ACS Nano, 2018, 12: 1242–1249
5 Zhang Y, Payne D T, Pang C L, et al. State-selective dynamics of TiO_2 charge-carrier trapping and recombination. J Phys Chem Lett, 2019, 10: 5265–5270